Chinese Chemical Letters 37 (2026) 111824

Contents lists available at ScienceDirect

Chinese Chemical Letters

journal homepage: www.elsevier.com/locate/cclet

Nonporous cavitand-crosslinked polymers: Harnessing deep cavities for efficient organic micropollutant removal from water

Yang Liang[a,1], Xiaojuan Zhou[a,1], Rui Wang[a,*], Julius Rebek Jr.[a,b], Yang Yu[a,*]

[a] Center for Supramolecular Chemistry & Catalysis and Department of Chemistry, College of Science, Shanghai University, Shanghai 200444, China
[b] Skaggs Institute for Chemical Biology and Department of Chemistry, The Scripps Research Institute, La Jolla, CA 92037, United States

ARTICLE INFO

Article history:
Received 16 July 2025
Revised 29 August 2025
Accepted 10 September 2025
Available online 11 September 2025

Keywords:
Water pollution
Organic micropollutant removal
Crosslinked polymer
Cavitand polymerization
Adsorption study
Nonporous polymer

ABSTRACT

Organic pollutants, a pivotal factor in water pollution, have persistently menaced the aquatic ecosystem, as well as the sustainable development of human health, economy, and society. Consequently, there is an urgent need for advanced techniques to efficiently eliminate organic micropollutants from water. Here, we present the synthesis of three nonporous cavitand-crosslinked polymers capable of adsorbing diverse organic pollutants from aqueous solutions. These polymeric adsorbents exhibit outstanding adsorptive performance towards the tested micropollutants, characterized by high apparent adsorption rate constants (k_{obs}) and maximum adsorption capacities ($q_{max,e}$). Notably, Compound **NCCP-1** demonstrated a remarkable $q_{max,e}$ of 459 mg/g for bisphenol A (BPA), ranking among the highest values reported for organic polymer adsorbents. In-depth investigation of the adsorption mechanism of the nonporous polymer revealed that it involves the recognition of pollutants by the deep cavities of the cavitand moieties and the interstitial spaces between them, primarily mediated by the hydrophobic effect. Furthermore, **NCCP-1** was applied *in situ* water purification simulations and was proven to maintain its removal efficiency over more than four cycles, highlighting its potential for practical applications in water treatment.

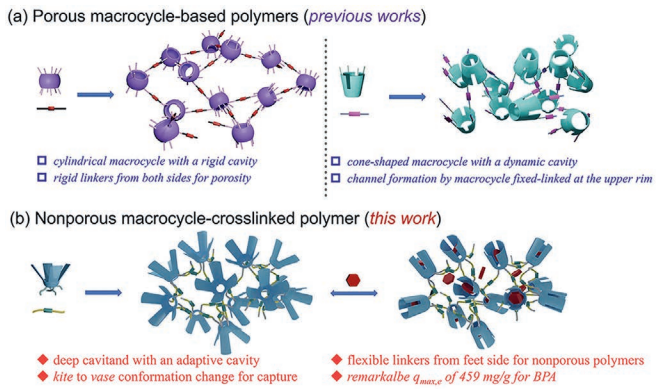
© 2025 Published by Elsevier B.V. on behalf of Chinese Chemical Society and Institute of Materia Medica, Chinese Academy of Medical Sciences.

Water pollution represents a preeminent threat to the safety and survival of life cycles on Earth, presenting a formidable challenge to the sustainable development of human health, the economy and society [1,2]. Anthropogenic organic chemicals, such as petroleum products, plasticizers, pesticides, pharmaceuticals, textile dyes and other industrial chemicals, have contaminated surface and groundwater, precipitating an environmental crisis that endangers the well-being of hundreds of millions of people [3]. In response, scientists have been actively developing diverse methods, including membrane filtration, flocculation, chemical oxidation and adsorption, to remove these predominantly non-biodegradable organic micropollutants from water. Among water purification treatment technologies, adsorption processes hold great promise due to their efficiency, versatility, and cost-effectiveness [4,5]. Activated carbon (AC) has long been the most popular and widely used adsorbent, owing to its effectiveness, scalability, high porosity, and substantial adsorption capacity [6–8]. However, AC has limitations, such as low affinity for relatively more polar pollutants and the requirement for harsh, energy-intensive regeneration procedures (heating up to 500–900 °C), and its original performance often cannot be fully restored. As such, there remains an urgent need for alternative adsorbents that can efficiently and renewably remove organic micropollutants from water.

In addition to traditional inorganic adsorbents, advanced organic materials have emerged as attractive alternatives because of their thermal stability and milder regeneration conditions. Porous organic polymers (POPs) have garnered significant attention in recent years, attributed to their inherent advantages, including good chemical and thermal stability, high and tunable porosity, low density, and excellent structural diversity and variability [9–12]. POPs are constructed entirely from organic materials through various network-forming reactions and can be classified into subclasses such as covalent organic frameworks (COFs) [13–16], hypercrosslinked polymers (HCPs) [17,18], porous aromatic frameworks (PAFs) [19], conjugated microporous polymers (CMPs) [20–23], and polymers of intrinsic microporosity (PIMs) [24]. Traditionally, POPs are typically built from two-dimensional planar building blocks, which, to some extent, restricts their structural diversity. For non-planar building blocks, tetra-substituted-methanes are mainly used and they lack additional functions beyond linkage. Recently, porous macrocycle-based polymers have been developed as

* Corresponding authors.
E-mail addresses: wangrui1990@shu.edu.cn (R. Wang), yangyu2017@shu.edu.cn (Y. Yu).
[1] These authors contributed equally to this work.

https://doi.org/10.1016/j.cclet.2025.111824
1001-8417/© 2025 Published by Elsevier B.V. on behalf of Chinese Chemical Society and Institute of Materia Medica, Chinese Academy of Medical Sciences.



Scheme 1. (a) Porous macrocycle-based polymers (*previous works*). (b) Nonporous macrocycle-crosslinked polymers (*this work*).

a new class of POPs, especially for the removal of organic micropollutants (Scheme 1a) [25–27]. By integrating a macrocycle host module into the network, these materials offer both diverse three-dimensional structures and host-guest encapsulation capabilities [28]. In 2016, the Dichtel group made a breakthrough by reporting a cross-linked β-cyclodextrin polymer that could rapidly adsorb various organic micropollutants from water, with sorption rate constants 15 to 200 times higher than those of other commercial adsorbents [29]. Since then, different macrocyclic hosts have been incorporated into cross-linked polymer adsorbents [30,31], including other cyclodextrins [32–36], calixarenes [37–42], pillararenes [43–46], calix[4]pyrroles [47], and amide naphthotubes [48]. High specific surface area is a key feature of these materials, and adsorbates are primarily captured and retained through their porosities. Therefore, the cross-linking of macrocycle-based POPs generally employs rigid linkers to create sufficient porosity through robust channels. For cylindrical macrocycles with rigid cavities, such as cyclodextrin and pillararene, both sides of the host have linking groups to construct channels from two directions. For cone-shaped macrocycles, like calix[4]arene and calix[4]pyrrole, linkage usually occurs on the upper-rim side, and the conformation of the host is fixed to form rigid channels.

Here, as depicted in Scheme 1b, we report the design and synthesis of nonporous macrocycle-crosslinked polymers using flexible linkers for the adsorption of organic micropollutants. Cavitand, which has rarely been involved in this research area, was selected as the macrocycle module, and the linkage was positioned on the "foot" side rather than the upper-rim side. This design preserves the integrity and independence of the cavity and its supramolecular function. The flexible "feet" of the cavitand and the flexible linkage prevent the formation of rigid channels, resulting in the nonporous nature of the polymer. Consequently, intrinsic porosity is no longer the dominant factor in adsorption; instead, the supramolecular function of the macrocycle host and the interval spaces between them serve as the sources of the adsorptive mechanism. Unlike previously reported polymers incorporating corn-shaped macrocycles, in which the host conformation is rigidly fixed to form robust channels, the cavitand modules in our polymer feature an adaptable cavity. Prior to the presence of guests, these modules assume a kite conformation. However, once guest pollutant molecules infiltrate the cavity, they undergo a transformation, adopting a vase conformation. The cavitand modules function like molecular tweezers, reversibly seizing pollutants from water. During the desorption processes, they proficiently release these captured pollutants, demonstrating their highly efficient and reversible adsorption-desorption behavior. Cavitands are deep, vase-shaped molecular containers based on a resorcin[4]arene core with covalently attached aromatic walls. They can bind a wide range of molecules [49–53] and have been extensively applied in molecular recognition, self-assembly processes and organic reaction regulation, both in their organic-soluble and water-soluble forms [54–61]. In previous reports, water-soluble cavitands were used in liquid/liquid separation of xylenes [62] and inter-phase selective adsorption of alkanes [63,64]. In this work, we utilize cavitand as the core linking module to construct nonporous macrocycle-crosslinked polymers and apply them to remove frequently-detected pollutants from water. The structures and properties of these polymers are comprehensively characterized and investigated. Adsorptive kinetics and isothermal studies confirm their excellent performance. The polymer adsorbent can be recycled multiple times without any loss of its adsorptive function upon regeneration and can be used for the simultaneous removal of multiple pollutants from water.

As shown in Fig. 1a, three different polymers (**NCCP-1**, **NCCP-2** and **NCCP-3**) were synthesized to explore the influence of the cavitand host itself and the linkers. The synthesis started from cavitand **S1a** and **S1b** (Figs. S1 and S5 in Supporting information), which were used to construct water-soluble containers [49–56]. This was achieved by treating the chlorinated "feet" with sodium azide. In comparison to cavitand **S1b**, the upper rim of cavitand **S1a** [59] is covalently bridged with hydrocarbon chain spacers. This modification rigidifies the open end, maintaining it in a receptive vase conformation and preventing it from unfolding into the unreceptive kite conformation. The new compounds were characterized with ^{1}H and ^{13}C NMR spectroscopy, high-resolution electrospray ionization mass spectrometry (ESI-HRMS), and Fourier transform infrared (FT-IR) spectrometry (Figs. 1b and c, Figs. S2–S4, S6–S8 in Supporting information). The polymerization of cavitand **S2** was accomplished through the "Click" reaction with diyne compounds (1,4-diethynylbenzene or 1,6-heptadiyne), which gave rise to the final cavitand-crosslinked polymer products in good yields (Fig. 1a). These products were then characterized by diverse analytical methods (Figs. 1b and c, Fig. 2; Figs. S10, S11, S13, S14 in Supporting information). In the FT-IR spectra (Fig. 1b), both azide-functionalized cavitand **S2a** and **S2b** display intense absorption peaks at approximately 2100 cm^{-1}, which can be attributed to the $-N_3$ group. Notably, this characteristic peak vanishes in the corresponding FT-IR spectra of polymer product **NCCP-1**, **NCCP-2** and **NCCP-3**. This observation indicates that the azide groups of the monomeric cavitands were completely converted during the "Click" reaction for polymerization. To further confirm the formation of the polymer products, solid-state cross-polarization magic angle spinning (CP/MAS) ^{13}C NMR spectroscopy was conducted (Fig. 1c). The signals of the cavitand backbone were all preserved, suggesting the recognition ability is retained in the polymers. Moreover, the characteristic signals at around 145 and 125 ppm correspond to the 3- and 4-positions of the triazole ring, respectively. These comprehensive characterization results provide strong evidence for the successful synthesis of the cavitand-crosslinked polymer products.

The polymers were subsequently subjected to thermogravimetric analysis (TGA) to assess their thermal stability. As illustrated in Fig. 2a, during the initial stage, the weights of the polymers gradually declined, presumably due to the loss of adsorbed water. The evident weight loss of the polymers commenced at approximately 400 °C, which can be ascribed to the decomposition of the polymers. The porosity of the polymers was characterized using N_2 gas adsorption/desorption experiments (Fig. 2b, Figs. S10 and S13 in Supporting information). The adsorption isotherms of the polymers could be categorized as type III, where multilayer adsorption occurs without the formation of a monolayer, and such isotherms are commonly observed on nonporous materials. This implies that the adsorption mechanism of the cavitand-crosslinked polymers does rely on their porosity but rather on the recognition and ad-

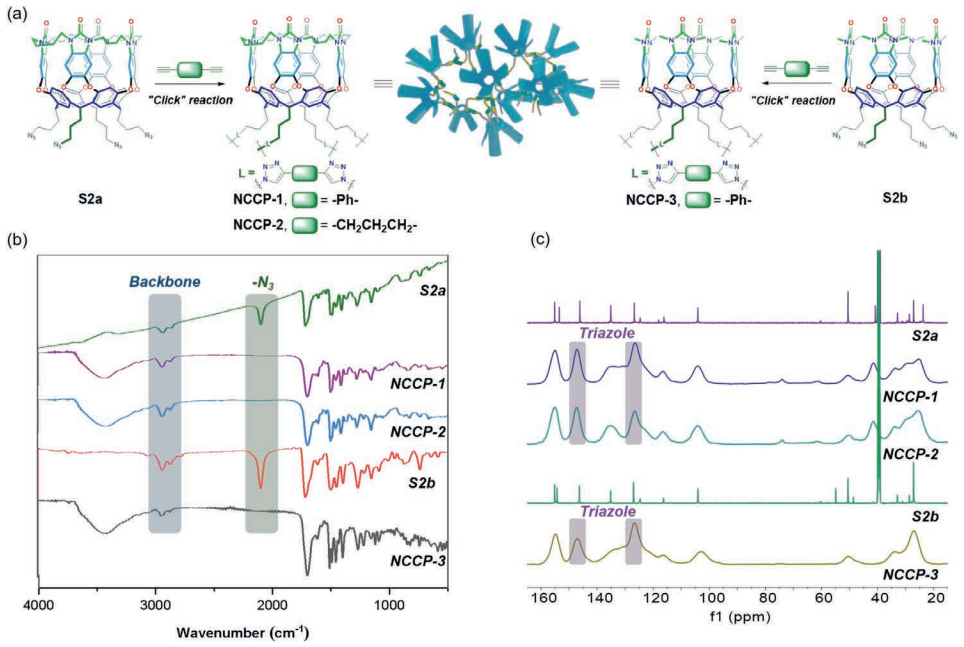


Fig. 1. (a) Synthesis of **NCCP-1**∼**3** and the cartoon illustration of the polymer structure. (b) FT-IR spectra of **S2a**, **S2b**, **NCCP-1**∼**3**. (c) ^{13}C NMR spectra of **S2a**, **S2b** and solid-state ^{13}C NMR spectra of **NCCP-1**∼**3**.

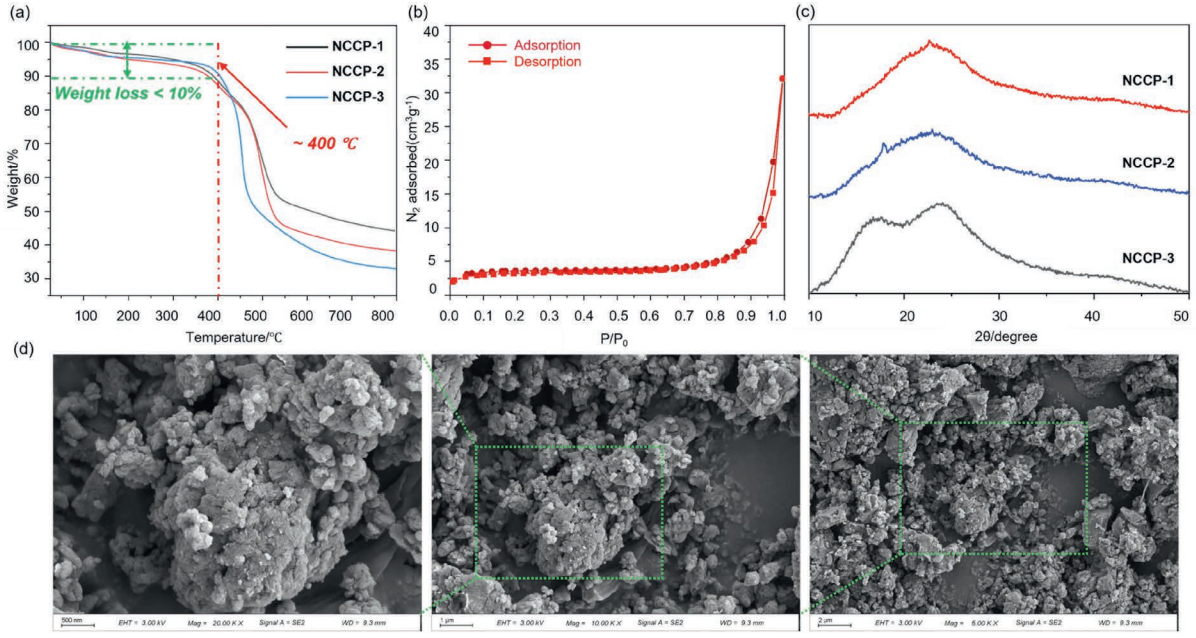


Fig. 2. (a) TGA curves of **NCCP-1**∼**3**. (b) N_2 adsorption and desorption curves of **NCCP-1**. (c) PXRD spectra of **NCCP-1**∼**3**. (d) SEM images of **NCCP-1**.

sorption of the adsorbates into the cavities of the cavitands and the inter-cavitand space. Furthermore, the Brunauer-Emmett-Teller (BET) surface areas were determined to be 12.3 m^2/g for **NCCP-1**, 10.7 m^2/g for **NCCP-2**, and 14.3 m^2/g for **NCCP-3**. These values also indicate the probable nonporous nature of the polymers. This may be attributed to the flexibility of the linkers, which disrupts the formation of channels within the polymer networks. In their powder X-ray diffraction (PXRD) spectra (Fig. 2c), all three polymers exhibited broaden signals, indicating their amorphous state in the solid state. This was further corroborated by scanning electron microscopy (Fig. 2d, Figs. S11 and S14 in Supporting information). All the polymers displayed dense amorphous particles, which also implies a nonporous characteristic. The particle sizes ranged from hundreds of nanometers to several micrometers, resulting in large solid-liquid contact surfaces that are conducive to the effective removal of organic micropollutants. The water regain values of **NCCP-1**, **NCCP-2** and **NCCP-3** were 13.6%, 5.8%, and 6.4%, respectively. These relatively low values also point to the probable nonporous feature of the polymers. To sum up, various characterizations have collectively demonstrated that the cavitand-crosslinked polymers are nonporous.

Five representative and frequently-encountered organic pollutants (Fig. 3a) were selected to test the adsorption ability of the polymer adsorbents: 1-naphthylamine (an aromatic model com-

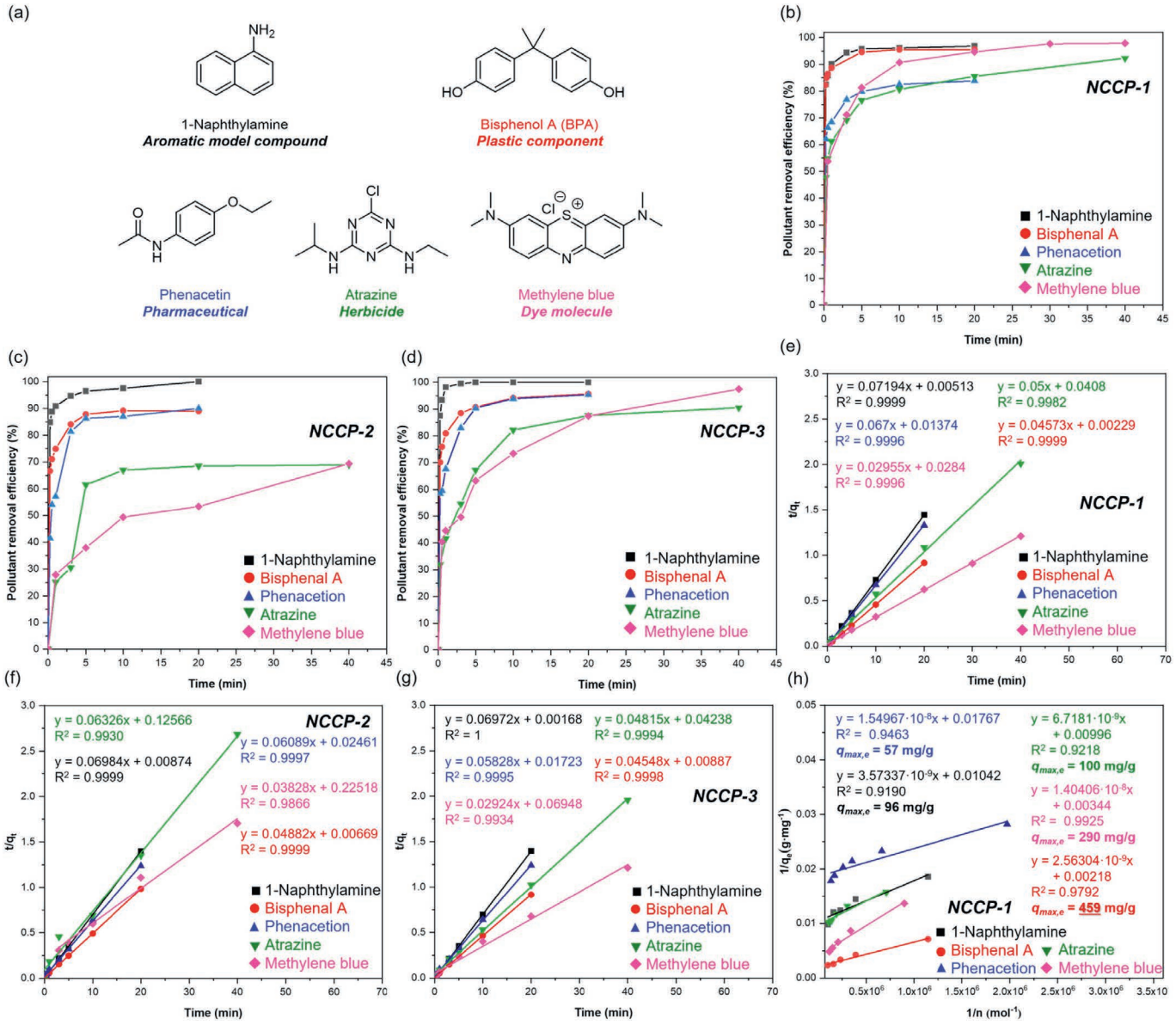


Fig. 3. (a) Structures and classification of the selected organic micropollutants. (b-d) Time-dependent removal efficiencies for the adsorptive removal of micropollutants by **NCCP-1**∼**3**. (e–g) Fits to the Ho and McKay's *pseudo*-second-order model for the adsorption of micropollutants by **NCCP-1**∼**3**. (h) Fits to the Langmuir adsorption isotherms for the adsorptive removal of micropollutants by **NCCP-1**.

pound), bisphenol A (BPA, a plastic component), phenacetin (a pharmaceutical), atrazine (a herbicide), methylene blue (a dye molecule). For the standard adsorption analysis, 3.0 mg of the polymer was added to 3.0 mL of a 0.10 mmol/L aqueous solution of the pollutant and stirred vigorously for a specific duration. After filtration, the filtrate was analyzed using UV–vis spectroscopy. The removal efficiency was calculated from absorbance changes relative to the stock solution, with calibration curves (Figs. S16–S20 in Supporting information). A qualitative assessment of the polymer adsorbents' adsorption abilities (Figs. 3b–d and Figs. S21–S23 in Supporting information) shows that all three polymer adsorbents could rapidly adsorb the pollutants within 1 h. From Figs. 3b–d, we can generally conclude qualitatively that polymer **NCCP-1** is the most effective in terms of both adsorption speed and capacity. The performance of **NCCP-2** and **NCCP-3** is relatively inferior, indicating that both the cavitand module and the linkage part play crucial roles in influencing the polymers' adsorptive capacity. More flexible and aliphatic linkers may affect the formation of adsorptive spaces between cavitand modules, and the host-guest interactions between the macrocycle module and the adsorbates are also significant. For all three polymers, pollutants such as BPA, 1-naphthylamine and phenacetin could be mostly adsorbed (>90%) very rapidly, within minutes and even seconds. This may be due to their relatively high hydrophobicity and affinity for the cavitand host.

To quantitatively compare the adsorption capabilities of the three polymers, the adsorption kinetic data were fitted using Ho and McKay's *pseudo*-second-order model [65]. Subsequently, the apparent adsorption rate constants [k_{obs} (g mg^{-1} min^{-1})] were determined (Figs. 3e–g and Figs. S24–S26 in Supporting information). The quantitative data were listed in Table 1. The results indicated that, on average, **NCCP-1** outperformed **NCCP-2** and **NCCP-3** in terms of removal efficiency, uptake q_e, and the apparent adsorption rate constant k_{obs}. Notably, **NCCP-1** also surpassed many previously reported adsorbents in terms of k_{obs}. Polymer **NCCP-1** was further subjected to adsorption studies at equilibrium. The equilib-

Table 1
Summary of binding constants (K_a) of micropollutants with **S3a**, **S3b** and apparent adsorption rate constants (k_{obs}) for the adsorptive removal of micropollutants by **NCCP1∼3** together with water solubility and logK_{ow} of micropollutants.

Micropollutants	K_a of **S3a** (L/mol)	K_a of **S3b** (L/mol)	k_{obs} of **NCCP-1** (g mg^{-1} min^{-1})	k_{obs} of **NCCP-3** (g mg^{-1} min^{-1})	k_{obs} of **NCCP-2** (g mg^{-1} min^{-1})	Solubility [a] (g/L)	logK_{ow} [b]
1-Naphthylamine	2.6×10^5	3.7×10^5	1.0080	2.8933	0.5580	0.97	2.25
BPA	–	–	0.9132	0.2331	0.3562	0.17	3.32
Phenacetin	1.6×10^5	4.0×10^4	0.3267	0.1971	0.1506	2.49	1.58
Atrazine	5.0×10^4	–	0.0612	0.0547	0.0318	0.21	2.61
Methylene blue	1.2×10^6	3.7×10^5	0.0307	0.0123	0.0065	43.60	0.75

[a] Water solubility data were taken from PubChem chemistry database.
[b] K_{ow} is the partition/distribution coefficient in *n*-octanol/water, and logK_{ow} data were taken from PubChem chemistry database.

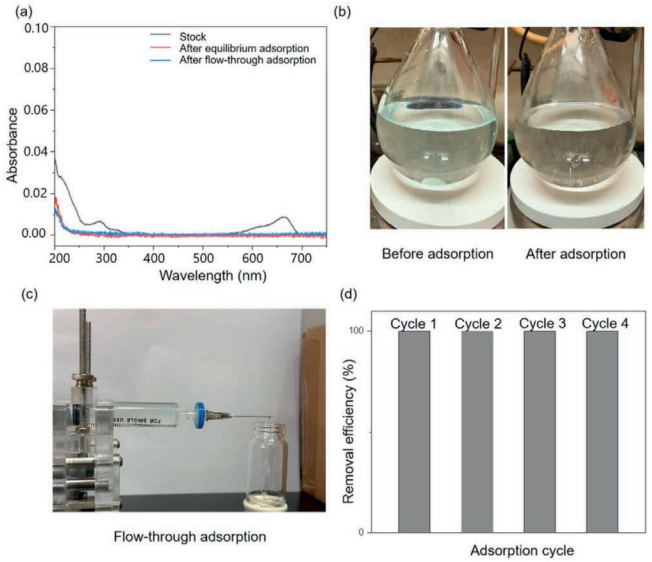


Fig. 4. (a) UV–vis absorption intensities of the mixture of 5 pollutants in deionized water at environmentally relevant concentration and after equilibrium and flow-through adsorption by **NCCP-1**. (b) Pictures of pollutant solutions before and after adsorption from (a). (c) Experimental setup for flow-through adsorption. (d) Removal efficiency of each circulative adsorption experiment of **NCCP-1** with BPA.

rium adsorption quantities of the micropollutants by **NCCP-1** increase with the increasing amount of adsorbates (Fig. 3h). The adsorption isotherms fit well to the Langmuir model [66]. The maximum adsorption capacity [$q_{max,e}$ (mg/g)] was calculated for each micropollutant (Fig. S27 in Supporting information), and the values are presented in Fig. 3h. The $q_{max,e}$ of BPA by **NCCP-1** is 459 mg/g, which is the highest among all reported nonporous materials. To the best of knowledge, it also ranks second among all reported macrocycle-crosslinked polymer adsorbents and third among all reported organic polymer materials.

To mimic the actual wastewater scenarios where multiple organic pollutants co-exist at environmentally relevant concentration (2.5–100 μg/L), a mixture of five pollutants (0.3 μmol/L for each one; *i.e.,* 43.0 μg/L 1-naphthylamine, 68.5 μg/L BPA, 53.8 μg/L phenacetin, 64.7 μg/L atrazine, 96.0 μg/L methylene blue) was tested. In a standard simultaneous adsorption experiment, 10.0 mg **NCCP-1** was pre-washed with 10.0 mL deionized water for 3 min and filtered. The washed **NCCP-1** was added to 300.0 mL abovementioned mixed solution and stirred vigorously at room temperature to reach equilibrium. After filtration, the filtrate was subjected to UV–vis spectroscopy. **NCCP-1** was shown to thoroughly adsorb all these pollutants (Fig. 4a), and the color of the pre-adsorbed solution changed from light blue to colorless (Fig. 4b). Impressively, this performance translates to a practical purification capacity of 1.0 g **NCCP-1** per 30.0 L wastewater, demonstrating significant potential of **NCCP-1** for *in situ* wastewater purification. At the same time, we conducted the flow-through adsorption experiment (Fig. 4c). 5.0 mg of the polymer was loaded onto the filter membrane and an injection pump was used to elute it with the abovementioned mixed solution at a rate of 12 mL/h. UV–vis analysis revealed complete elimination of all target micropollutants, as evidenced by the absence of characteristic absorption peaks. The color of the solution also faded after the filter membrane. Based on the experimental results, our polymers may offer a promising solution for rapid removal of multiple organic micropollutants coexist at environmentally relevant concentration of natural pollutant solutions. Subsequently, the recycling performance of **NCCP-1** was evaluated. After the standard adsorption process with BPA, **NCCP-1** was filtered. The collected solid was then vigorously stirred in EtOH at 50 °C for 12 h. Following filtration, the desorbed polymer was recovered, thoroughly dried under vacuum, and then reused for the next adsorptive cycle. The regenerated adsorbent exhibited nearly quantitative removal efficiency. Even after four adsorption-desorption cycles, the adsorbent retained its original efficiency for BPA removal (Fig. 4d and Fig. S28 in Supporting information).

As demonstrated above, the new polymers are classified as nonporous. This implies that the cavitand host sites and the inter-cavitand spaces are likely to be pivotal in governing their adsorption capabilities. To elucidate the role of cavitand modules within the polymer adsorbents, we probed the binding behaviors of the corresponding water-soluble cavitands towards organic pollutants in an aqueous medium. By mixing the water-soluble host (**S3a**, **S3b,** see Fig. S15 in Supporting information for details) and pollutant guest in 1:1 ratio and comparing the changes of the host signals in ^{1}H NMR spectra (Figs. S29–S38 in Supporting information), we found cavitand **S3a** could strongly bind atrazine, 1-naphthylamine, phenacetin and methylene blue. Similarly, **S3b** could strongly bind 1-naphthylamine, phenacetin and methylene blue. Isothermal titration calorimetry (ITC) titrations were then carried out to determine the binding constants (K_a) quantitatively (Figs. S39 and 40 in Supporting information), which are listed in Table 1 along with the k_{obs} data of the corresponding cavitand-crosslinked polymers for comparison. The binding thermodynamic parameters ($\Delta H^{\odot}$ and $-T\Delta S^{\odot}$) were also recorded. The results indicated that the binding between hosts and guests is generally enthalpically driven, with either favorable or unfavorable entropic contributions (Tables S1–S8 in Supporting information). Among the two cavitand hosts, a higher K_a value was often associated with a higher k_{obs} value for the corresponding polymer. For example, the K_a of 1-naphthylamine with **S3a** and **S3b** were 2.6×10^5 and 3.7×10^5 L/mol, respectively. Correspondingly, the k_{obs} of 1-naphthylamine for **NCCP-1** and **NCCP-3** were 1.0080 and 2.8933 g mg^{-1} min^{-1}, respectively. Similar trends were also observed among different pollutant compounds. For example, the K_a of 1-naphthylamine and phenacetin with **S3a** were 2.6×10^5 and 1.6×10^5 L/mol, respectively; while the k_{obs} of 1-naphthylamine and phenacetin for **NCCP-1** were 1.0080 and 0.3267 g mg^{-1} min^{-1}, respectively. These trends strongly suggest that the cavitand moieties within the polymer play a cruical role in adsorbing microp-

ollutants through host-guest recognition. However, the counterexamples observed for methylene blue compared to other pollutants (highlighted in green) and the series of **S3a**-containing polymer **NCCP-2** (highlighted in blue) indicate the host-guest interaction is not the sole determinant of the polymers' adsorption ability. Another factor is the inter-cavitand spacing created by the linkers. It is well known that host macrocycles bind guest molecules through a variety of noncovalent interactions. Pollutant molecules may also be adsorbed into the spaces between cavitand units and the linkers *via* similar recognition processes. For example, **NCCP-2** shares the same cavitand as **NCCP-1** but has a different linker. As a result, it exhibits distinct and inferior adsorption performance. This implies that the linker also plays a role in the adsorption behavior of the polymer. Compared to the aromatic linker of **NCCP-1**, the aliphatic linker of **NCCP-2** is more flexible and prone to folding, which may reduce the inter-cavitand space. Additionally, its aliphatic nature weakens the attraction for pollutant molecules to enter the interval spaces of the polymer. Furthermore, hydrophobicity is also a considerable factor (the water solubility and logK_{ow} values of each pollutant are also integrated into Table 1). Hydrophobic pollutants are forced from the aqueous phase into the interior of the polymer, and their expulsion from water accelerates the adsorption process. The binding constants of methylene blue with **S3a** and **S3b** are relatively high, yet its corresponding adsorption rate constants are comparatively low. This could be attributed to the dye's high water solubility (43.60 g/L, log$K_{ow} = 0.75$), which weakens the hydrophobic driving force. To summarize, given the nonporous nature of our polymers, three primary factors influence their adsorption abilities: (1) The cavitand host sites dispersed within the polymers can bind the pollutant molecules within their cavities through host-guest recognition, as evidenced by the positive correlation between k_{obs} and K_a values in most cases; (2) The spaces created by the linkers between cavitand modules can also bind and adsorb pollutants through non-covalent interactions, which explains the counterexamples and the different adsorption abilities between **NCCP-1** and **NCCP-2**; (3) Hydrophobicity can also serve as a driving force for the adsorption process, as exemplified by the reduced k_{obs} for methylene blue. These three factors jointly determine the adsorption capacity of cavitand-cross linked polymer adsorbents.

In conclusion, three nonporous cavitand-crosslinked polymer adsorbents were synthesized and characterized. These polymer adsorbents exhibited excellent adsorptive performance towards representative and commonly detected organic pollutants, such as 1-naphthylamine, bisphenol A (BPA), phenacetin, atrazine and methylene blue. The removal efficiencies of the polymers for micropollutants reached as high as >99 %, and their adsorptive kinetics and isotherms were systematically investigated. The apparent adsorption rate constants (k_{obs}) and the maximum adsorption capacity ($q_{max,e}$) of **NCCP-1** for the tested micropollutants surpassed those of most previously reported adsorbents. Notably, the $q_{max,e}$ for BPA is 459 mg/g, which, to the best of our knowledge, is the highest among reported nonporous materials and is comparable to the top-performing organic polymer adsorbents. Our studies revealed that the high performance of these adsorbents stems from the recognition by cavitands, adsorption into the interstices, and hydrophobic effects. Significantly, these adsorbents could efficiently adsorb mixtures of different pollutant families from water at environmentally relevant concentration in flow-through manner. The new adsorbents could be readily regenerated by treatment with EtOH and reused for over four cycles without any loss of efficiency. These results suggest that nonporous organic polymers based on macrocycle host molecules hold great promise for the research and applications of adsorption processes, particularly for the removal of diverse organic micropollutants from wastewater.

Declaration of competing interest

The authors declare that they have no known competing financial interests or personal relationships that could have appeared to influence the work reported in this paper.

CRediT authorship contribution statement

Yang Liang: Software, Investigation, Formal analysis, Data curation. **Xiaojuan Zhou:** Software, Methodology, Investigation. **Rui Wang:** Writing – review & editing, Writing – original draft, Supervision, Methodology, Investigation, Funding acquisition, Formal analysis, Conceptualization. **Julius Rebek Jr.:** Writing – review & editing, Visualization. **Yang Yu:** Writing – review & editing, Writing – original draft, Supervision, Project administration, Funding acquisition, Conceptualization.

Acknowledgments

This work was supported by the National Natural Science Foundation of China (Nos. 22322107, 22101169 and 22071144) and by Shanghai Scientific and Technological Committee (No. 22010500300).

Supplementary materials

Supplementary material associated with this article can be found, in the online version, at doi:10.1016/j.cclet.2025.111824.

References

[1] R.P. Schwarzenbach, T. Egli, T.B. Hofstetter, et al., Rev. Environ. Res. 35 (2010) 109–136.
[2] M. Stuart, D. Lapworth, E. Crane, et al., Sci. Total Environ. 416 (2012) 1–21.
[3] R.P. Schwarzenbach, B.I. Escher, K. Fenner, et al., Science 313 (2006) 1072–1077.
[4] Y. Luo, W. Guo, H.H. Ngo, et al., Sci. Total Environ. 473 (2014) 619–641.
[5] M.O. Barbosa, N.F.F. Moreira, A.R. Ribeiro, et al., Water Res. 94 (2016) 257–279.
[6] J. Orfao, A. Silva, J. Pereira, et al., J. Colloid Interf. Sci. 296 (2006) 480–489.
[7] E.K. Putra, R. Pranowo, J. Sunarso, et al., Water Res. 43 (2009) 2419–2430.
[8] L. Kovalova, D.R.U. Knappe, K. Lehnberg, et al., Environ. Sci. Pollut. Res. 20 (2013) 3607–3615.
[9] P. Kaur, J.T. Hupp, S.T. Nguyen, ACS Catal. 1 (2011) 819–835.
[10] W. Chen, P. Chen, G. Zhang, et al., Chem. Soc. Rev. 50 (2021) 11684–11714.
[11] Z. Li, Y.W. Yang, Adv. Mater. 34 (2021) 2107401.
[12] M.G. Mohamed, A.F.M. EL-Mahdy, M.G. Kotpa, et al., Mater. Adv. 3 (2022) 707–733.
[13] A.P. Côté, A.I. Benin, N.W. Ockwig, et al., Science 310 (2005) 1166–1170.
[14] J. Chen, Y. Wang, Y. Yu, et al., Exploration 3 (2023) 20220144.
[15] L. Guan, D. Mehdi, H. Li, et al., Chin. Chem. Lett. 36 (2025) 111389.
[16] Y.H. Jin, M.H. Li, Y.W. Yang, Adv. Sci. 12 (2025) 2412600.
[17] L. Tan, B. Tan, Chem. Soc. Rev. 46 (2017) 3322–3356.
[18] P. Liu, C. Long, H.M. Qian, et al., Chin. Chem. Lett. 20 (2009) 492–495.
[19] B. Li, Y. Zhang, R. Krishna, et al., J. Am. Chem. Soc. 136 (2014) 8654–8660.
[20] Y. Xu, S. Jin, H. Xu, A. Nagaia, et al., Chem. Soc. Rev. 42 (2013) 8012–8031.
[21] L. Liu, K. Dong, M. Hassan, et al., Green Synth. Catal. 3 (2022) 349–356.
[22] K. Wang, R. Fan, X. Wei, et al., Green Synth. Catal. 3 (2022) 327–338.
[23] X. Li, Z. Li, Y.W. Yang, Adv. Mater. 30 (2018) 1800177.
[24] N.B. McKeown, P.M. Budd, Chem. Soc. Rev. 35 (2006) 675–683.
[25] M.J. Klemes, L.P. Skala, M. Ateia, et al., Acc. Chem. Res. 53 (2020) 2314–2324.
[26] X. Ji, H. Wang, H. Wang, et al., Angew. Chem. Int. Ed. 59 (2020) 23402–23412.
[27] T. Skorjanc, D. Shetty, A. Trabolsi, Chem 7 (2021) 882–918.
[28] Y. Li, X. Lou, C. Wang, et al., Chin. Chem. Lett. 34 (2023) 107877.
[29] A. Alsbaiee, B.J. Smith, L. Xiao, et al., Nature 529 (2016) 190–194.
[30] D.J. Fortman, J.P. Brutman, G.X. De Hoe, et al., ACS Sustain. Chem. Eng. 6 (2018) 11145–11159.
[31] B.R. Elling, W.R. Dichtel, ACS Cent. Sci. 6 (2020) 1488–1496.
[32] D.M. Alzate-Sanchez, B.J. Smith, A. Alsbaiee, et al., Chem. Mater. 28 (2016) 8340–8346.
[33] L. Xiao, Y. Ling, A. Alsbaiee, et al., J. Am. Chem. Soc. 139 (2017) 7689–7692.
[34] Y. Ling, M.J. Klemes, L. Xiao, et al., Environ. Sci. Technol. 51 (2017) 7590–7598.
[35] M.J. Klemes, Y. Ling, C. Ching, et al., Angew. Chem. Int. Ed. 58 (2019) 12049–12053.
[36] F. Tong, Y. Zhou, Y. Xu, et al., Exploration 3 (2023) 20210111.
[37] D. Shetty, I. Jahovic, J. Raya, et al., J. Mater. Chem. 5 (2017) 62–66.
[38] D. Shetty, J. Raya, D.S. Han, et al., Chem. Mater. 29 (2017) 8968–8972.
[39] D. Shetty, J. Jahovic, J. Raya, et al., ACS Appl. Mater. Interfaces 10 (2018) 2976–2981.

[40] Z. Zheng, H. Yu, W. Geng, et al., Nat. Commun. 10 (2019) 5762.
[41] D. Shetty, I. Jahovic, T. Skorjanc, et al., ACS Appl. Mater. Interfaces 12 (2020) 43160–43166.
[42] D. Shetty, S. Boutros, T. Skorjanc, et al., J. Mater. Chem. A 8 (2020) 13942–13945.
[43] B. Shi, H. Guan, L.Q. Shangguan, et al., J. Mater. Chem. A 5 (2017) 24217–24222.
[44] S. Lan, S. Zhan, J. Ding, et al., J. Mater. Chem. A 5 (2017) 2514–2518.
[45] Q. Zhao, Y. Liu, Chem. Commun. 54 (2018) 7362–7365.
[46] G. Zhang, X.Y. Lou, M.H. Li, et al., Dyes Pigm. 206 (2022) 110576.
[47] X. Wang, L. Xie, K. Lin, et al., Angew. Chem. Int. Ed. 60 (2021) 7188–7196.
[48] L.P. Yang, H. Ke, H. Yao, et al., Angew. Chem. Int. Ed. 60 (2021) 21404–21411.
[49] B. Purse, J. Rebek Jr., Pror. Natl. Acad. Sci. U. S. A. 102 (2005) 10777–10782.
[50] R.J. Hooley, J. Rebek Jr., Chem. Bio. 16 (2009) 255–264.
[51] D. Ajami, J. Rebek Jr., Acc. Chem. Res. 46 (2013) 990–999.
[52] D. Ajami, L. Liu, J. Rebek Jr., Chem. Soc. Rev. 44 (2015) 490–499.
[53] F.Y. Chen, W.C. Geng, K. Cai, et al., Chin. Chem. Lett. 35 (2024) 109161.
[54] S.M. Biros, J. Rebek Jr., Chem. Soc. Rev. 36 (2007) 93–104.
[55] K.D. Zhang, D. Ajami, J.V. Gavette, et al., J. Am. Chem. Soc. 136 (2014) 5264–5266.
[56] Y. Yu, J. Rebek Jr., Acc. Chem. Res. 51 (2018) 3031–3040.
[57] Y. Yu, J.M. Yang, J. Rebek Jr., Chem 6 (2020) 1265–1274.
[58] Y. Yu, J. Rebek Jr., Q. Rev. Biophys. 53 (2020) e6.
[59] J.M. Yang, Y.Q. Chen, Y. Yu, et al., J. Am. Chem. Soc. 143 (2021) 19517–19524.
[60] M. Petroselli, Y.Q. Chen, J. Rebek Jr., et al., Green Synth. Catal. 2 (2021) 123–130.
[61] R. Wang, Y. Liang, J. Rebek Jr., et al., Chin. Chem. Lett. 35 (2024) 109228.
[62] F.U. Rahman, J. Yang, Y.M. Wan, et al., Chem. Commun. 56 (2020) 6945–6948.
[63] S. Saito, J. Rebek Jr., Bioorg. Med. Chem. Lett. 11 (2001) 1497–1499.
[64] Y.H. Wan, F.U. Rahman, J. Rebek Jr., et al., Chin. J. Chem. 39 (2021) 1498–1502.
[65] Y.S. Ho, G. McKay, Process Biochem. 34 (1999) 451–465.
[66] I. Langmuir, J. Am. Chem. Soc. 40 (1918) 1361–1403.